LASER SURFACE HARDENING OF AISI 1055 STEEL IN WATER-SUBMERGED CONDITION

NIROJ MAHARJAN[1, 2], WEI ZHOU[1,*], YU ZHOU[2] and NAIEN WU[3]

[1]*School of Mechanical and Aerospace Engineering, Nanyang Technological University, 50 Nanyang Avenue, Singapore 639798*

[2]*Advanced Remanufacturing and Technology Centre, 3 CleanTech Loop, Singapore 637143*

[3]*Precision Laser Solutions Pte. Ltd, 280 Woodlands Industrial Park E5, Singapore 757322*

* Corresponding author

E-mail address: wzhou@cantab.net; *Tel:* +65 6790 4700

Underwater laser hardening might produce better surface mechanical properties than conventional laser hardening in air due to additional cooling effect by water. However, it has not been studied in detail. This study investigates the effect of water layer on laser surface hardening of AISI 1055 steel. It is found that laser surface hardening is feasible with water layer up to 3 mm above the steel surface. A higher surface hardness is achieved during underwater processing. This is attributed to fast cooling by water which facilitates complete martensitic transformation. Nevertheless, the hardened area is smaller than that in conventional laser hardening in air due to attenuation of laser energy. Above 3 mm, the laser beam is severely attenuated due to formation of vapor plume. Furthermore, it is found that surface oxidation cannot be prevented completely even during underwater treatment, and the water movement results in random distribution of metal slag on the surface.

Keywords: laser surface hardening; water cooling; hardness; steel.

1. Introduction

Laser-based surface processing is increasingly being employed in industries to modify the surface properties of materials.[1–5] Laser surface hardening is one of such selective heat treatment processes that produces a hard wear resistant layer without affecting the bulk properties of steel.[6] It uses heating from the laser beam to quickly austenitize the surface. When the laser beam moves away, the heated surface cools rapidly, leading to formation of martensitic microstructure with higher hardness than the bulk material.[7]

The phase transformation during laser surface hardening is primarily dictated by peak temperature, dwell time and cooling rate. Higher cooling rate increases the chance of complete martensitic transformation.[8] Since water has high specific heat capacity, it might produce additional cooling effect during laser hardening process. However, little attention is paid in literature to exploit the beneficial effect of water layer during laser surface hardening.

Extensive studies have been performed to investigate the effect of water in underwater laser welding for basic repair and joining in offshore structures such as submerged pipelines, oil platforms and other submerged structures.[9–11] These studies show that water has significant effect on the weld morphology and strength. Similar effect is expected during laser surface hardening in submerged condition since both welding and surface hardening are basically heating processes. Under proper water depth, water submerged laser hardening treatment might produce superior surface characteristics that is remarkably different from laser hardening in air.

Therefore, the effect of water layer on hardness and surface properties of steel during laser hardening is explored in this study. Laser hardening of AISI 1055 steel is carried out both in air and water. The obtained results are analyzed based on the hardness and the size of hardened area. In addition, the effect of water environment on surface morphology and oxidation is also presented.

2. Materials and methods

The material used for the study was AISI 1055 steel which is a medium carbon steel used in automobile components such as gears, axles and clutches as well as in heavy forging applications. The nominal chemical composition of the steel is shown in Table 1. The original material was received as a rolled plate from which specimens of 50 × 25 × 10 mm^3 were extracted. The surface of specimen was ground on progressively finer grades of emery papers up to P1200 grit size. The average surface roughness after grinding was about 0.4 μm. The ground surface was then cleaned with ethanol and dried with an air gun before performing the laser treatment.

Table 1. Chemical composition (in wt%) of AISI 1055 steel used.

Elements	C	Cr	Mn	Si	P	S	Ni	Cu	B	Fe
wt%	0.56	0.11	0.78	0.23	0.01	0.002	0.07	0.06	0.0015	Balance

An Ytterbium based fiber laser (YLR-150/1500-QCW IPG Photonics) was utilized to harden the surface. The experimental setup is shown in Fig. 1. The laser produced IR beam of wavelength 1.07 μm and had a nominal power of 250 W in continuous mode. The beam was delivered through optical fiber and a lens of 300 mm focal length was used to focus the beam. A defocus distance of 10 mm was maintained for all experiments. Series of line scans were drawn on the surface of the specimen at different laser processing parameters (see Table 2) using a Galvanometric scanner (from SCANLAB). The specimen was completely submerged in water with varying thickness of water layer above the surface. Experiments were also carried out in air to compare the hardening results from water submerged conditions.

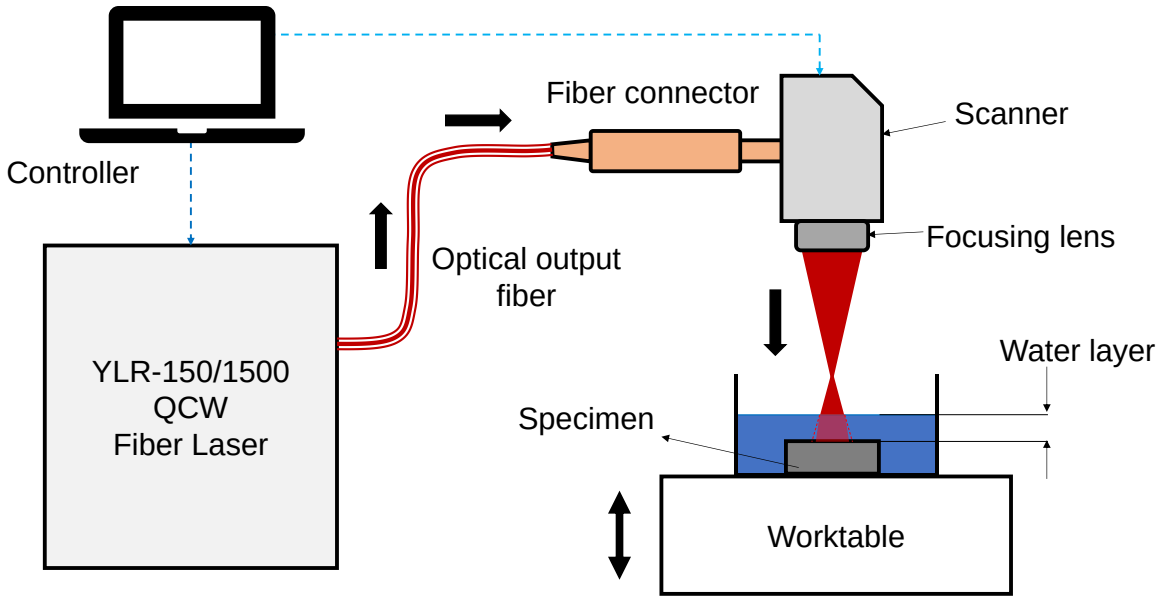

Fig. 1. Schematic diagram showing experimental setup for underwater laser hardening.

Table 2. Experimental conditions used for hardening trials.

Parameters	**Condition/Range**
Water layer thickness	0 (air), 1, 3, 5 mm
Laser power (W)	250 W
Traverse speed (mm/s)	1, 5, 10, 25, 50, 75, 100 mm/s

The surface morphology of the laser treated specimen was analyzed using optical microscopy (Olympus SZX16 and Carl Zeiss Axioskop 2) and electron microscopy (JEOL 5600LV and JEOL 7600F equipped with INCA X-Stream EDS). In order to study the cross-section microstructure, transverse section was made across the scan line using abrasive cutter. The cut sample was mounted, ground and polished using standard metallographic sample preparation technique. After final polishing with 0.04 μm colloidal silica suspension, a 2% nital (2% HNO_3 + 98% C_2H_5OH) etching was performed on the polished surface to reveal the hardened microstructure. Moreover, a microvickers

hardness indenter (FutureTech FM300e) was implemented to measure the surface and cross-section hardness. It used a 300 gf (for surface measurements) and 100 gf (for cross-section measurements) load at 15 s dwell time.

3. Results and Discussion

Figure 2 presents typical hardened line tracks under various water depths. A constant laser power of 250 W and traverse speed of 10 mm/s was used to produce these line tracks. As can be seen, the formation of scan line worsens with increase in water depth. The scan track becomes almost invisible when the water depth is ≥ 5 mm. In addition, it is also observed that the width of scan track becomes small and zigzag with increase in water depth.

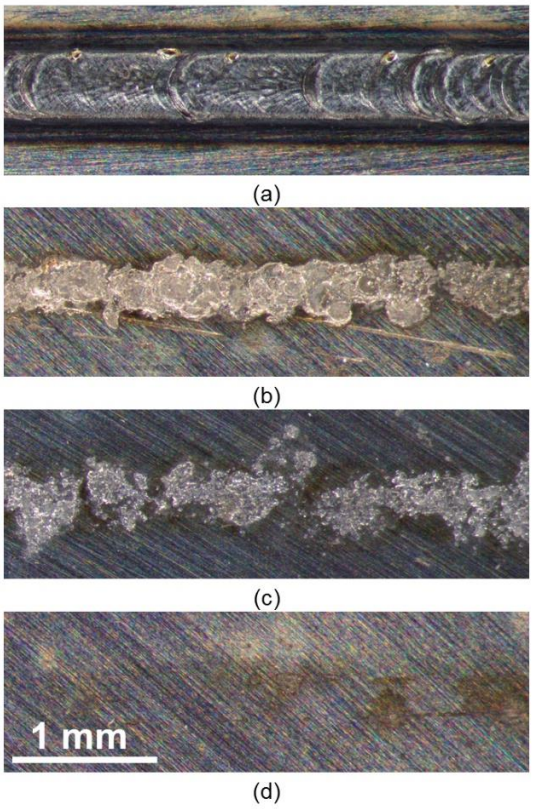

Fig. 2. Images showing laser hardened surfaces at different water layer – (a) 0 mm (air); (b) 1 mm; (c) 3 mm; and (d) 5 mm.

Further analysis of the hardened surface with SEM and EDS revealed presence of oxygen. Figures 3 and 4 show element maps of surfaces treated in air and water respectively. In case of laser treatment in air, the oxide scale was uniformly distributed all over the hardened surface as evidenced by presence of oxygen in the scan track (see Fig. 3(c)). Several bumps were observed at the edge of the hardened track which was identified as metal slag made up of Fe, O, Mn, Si and C. The affinity of alloying elements with oxygen must have resulted in segregation at the surface during laser heating and formed these bumps.[12] On the other hand, the water submerged laser treated surface did not exhibit a uniform oxide layer. Instead, the oxygen was concentrated in the metal slag (see Fig. 4(c)). The metal slag was distributed randomly over the hardened surface due to the movement of water during laser hardening.

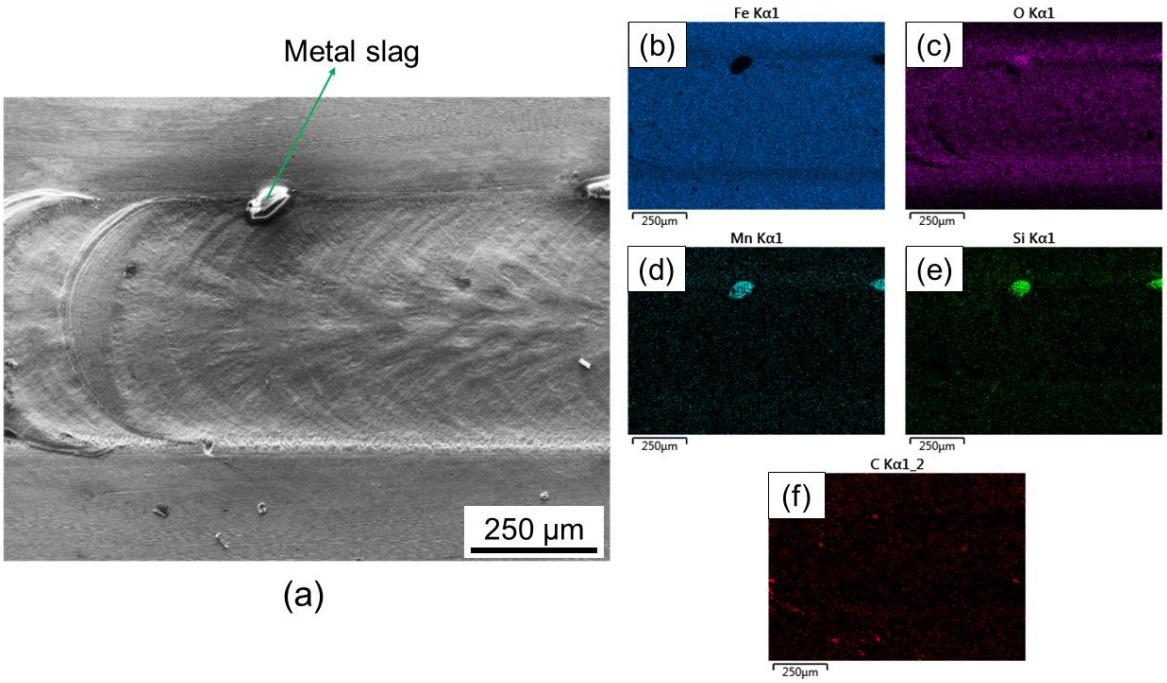

Fig. 3. Surface maps during laser hardening in air at 250 W power and 10 mm/s traverse speed – (a) electron image; (b) Fe map; (c) O map; (d) Mn map; (e) Si map; and (f) C map.

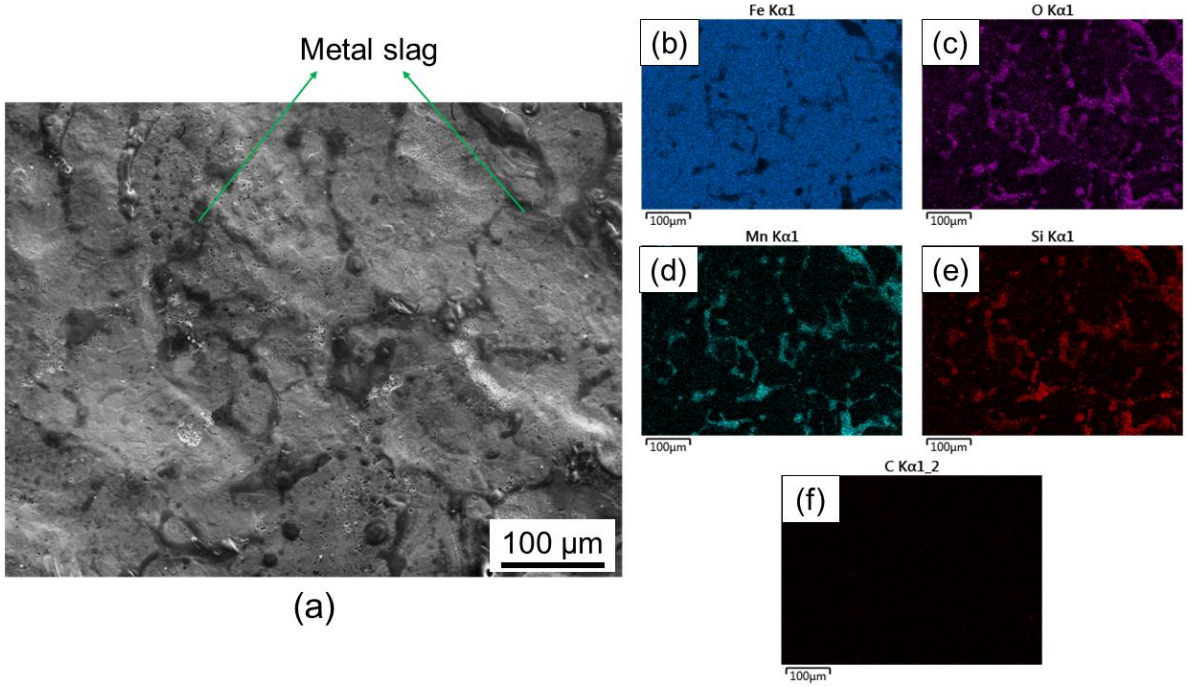

Fig. 4. Surface maps during laser hardening under water (1 mm thick water layer) at 250 W power and 10 mm/s traverse speed – (a) electron image; (b) Fe map; (c) O map; (d) Mn map; (e) Si map; and (f) C map.

The results thus demonstrate the effect of water layer on morphologies of hardened surfaces. It is found that the surface oxidation persists despite having a protective water layer over the steel surface. The presence of water layer significantly attenuates the laser energy reaching the steel surface producing smaller hardened track than in air. The extent of attenuation depends on the thickness of water layer. Although theoretical analysis calculated only about 13.1% of the total laser energy is absorbed by water layer as thick as 10 mm,[13] the obtained results exhibit drastic reduction in size of hardened track even with 5 mm water layer (see Fig. 2(d)). This can be explained by formation of plasma plume and water vapor cloud.

A bright plasma was observed during water submerged hardening experiments as shown in Fig. 5. When the steel surface is irradiated by the laser beam in air, the surface is heated up quickly to a high temperature and forms hardened structure on rapid cooling (see Fig. 6(a)). In presence of water, evaporation of water forms vapor cloud over the surface. The vapor cloud causes attenuation of energy reaching the surface.[9] When the water layer is thin, the laser energy is high enough to vaporize a small water channel along the beam path (see Fig. 6(b)) delivering enough energy onto the surface.[10] However, when the water layer is thick (> 3 mm), the plasma forming at the steel surface is confined by the water pressure. This severely blocks the laser energy from reaching the surface (see Fig. 6(c)). The plume is unstable and as the laser beam moves away, it is rapidly flooded by water. This creates random motion of water producing zigzag scan track and non-uniform distribution of metal slag.

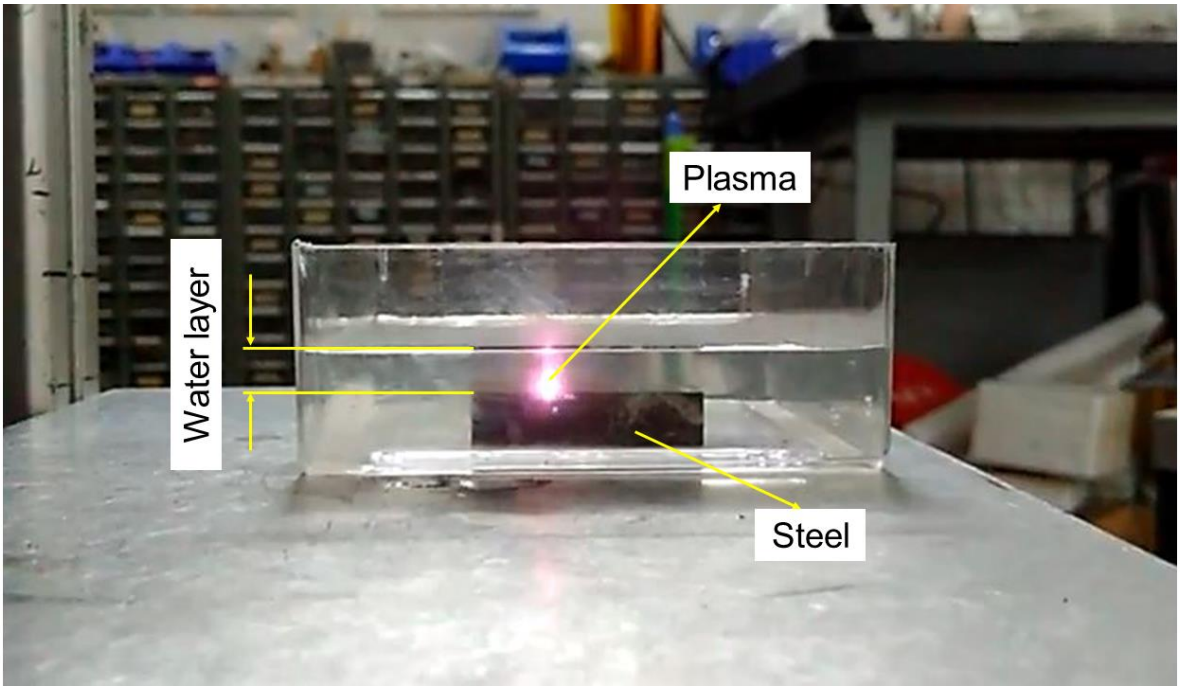

Fig. 5. Image showing plasma formation during water submerged laser hardening process.

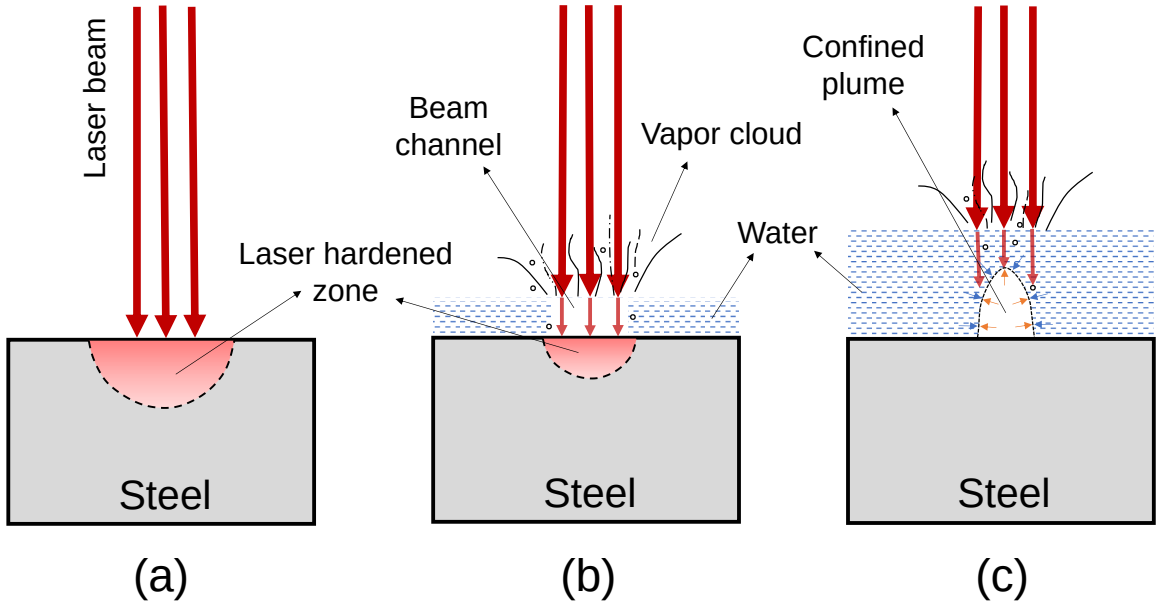

Fig. 6. Illustration showing laser hardening process (a) in air; (b) with thin layer of water; and (c) with thick layer of water.

Figure 7 shows the variation of surface hardness with change in traverse speed for both water submerged and air treated condition. A water layer of 1 mm was used for water submerged cases. It is found that the surface hardness of water submerged specimen is higher than air hardened specimen for all speeds. This suggests the beneficial effect of using water above the surface.

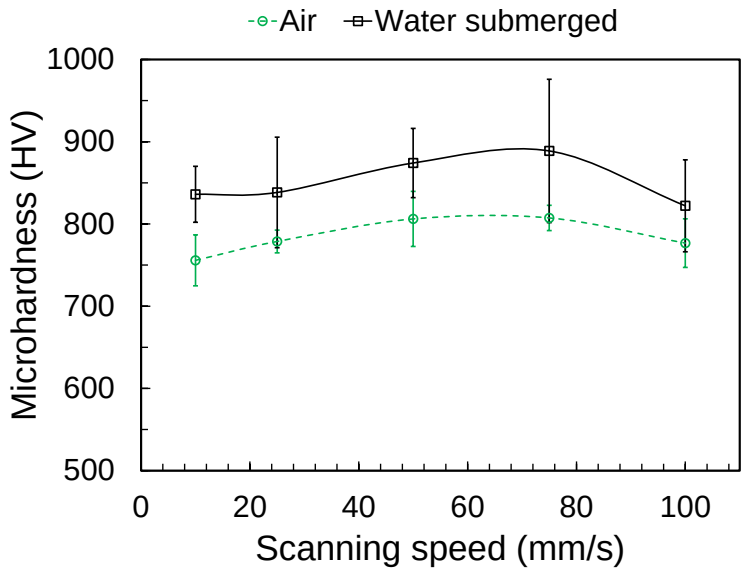

Fig. 7. Graph showing variation of surface hardness with traverse speed. Both conditions employed a constant laser power of 250 W.

The transverse section of the laser treated specimen was analyzed to further investigate the effect of water on the microstructure. Similar microstructures were obtained for both water submerged and air treated condition. Figure 8 shows a typical microstructure obtained at 250 W power and 10 mm/s traverse speed with 1 mm water layer. The base microstructure consisted of pearlite and pro-eutectoid ferrite as shown in Fig. 8(c). After laser treatment, martensite appeared in the laser hardened zone similar to conventional laser hardening in air (see Fig. 8(a)). The formation of martensite verifies rapid heating of the surface above austenitization temperature followed by fast cooling due to transfer of heat to the bulk of the specimen and water on the surface.[14] Away from the surface, the boundary region of the laser hardened zone had patches of pro-eutectoid ferrite in the matrix of austenite (see Fig. 8(b)). The temperature in this region is greater than Ac1 temperature, but lower than the Ac3 temperature. Therefore, the pearlite lamellae in the original microstructure dissolve and form austenite. However, the carbon cannot diffuse into the pro-eutectoid ferrite region due to low heating effect and less interaction time leaving the ferrite patches behind.[15]

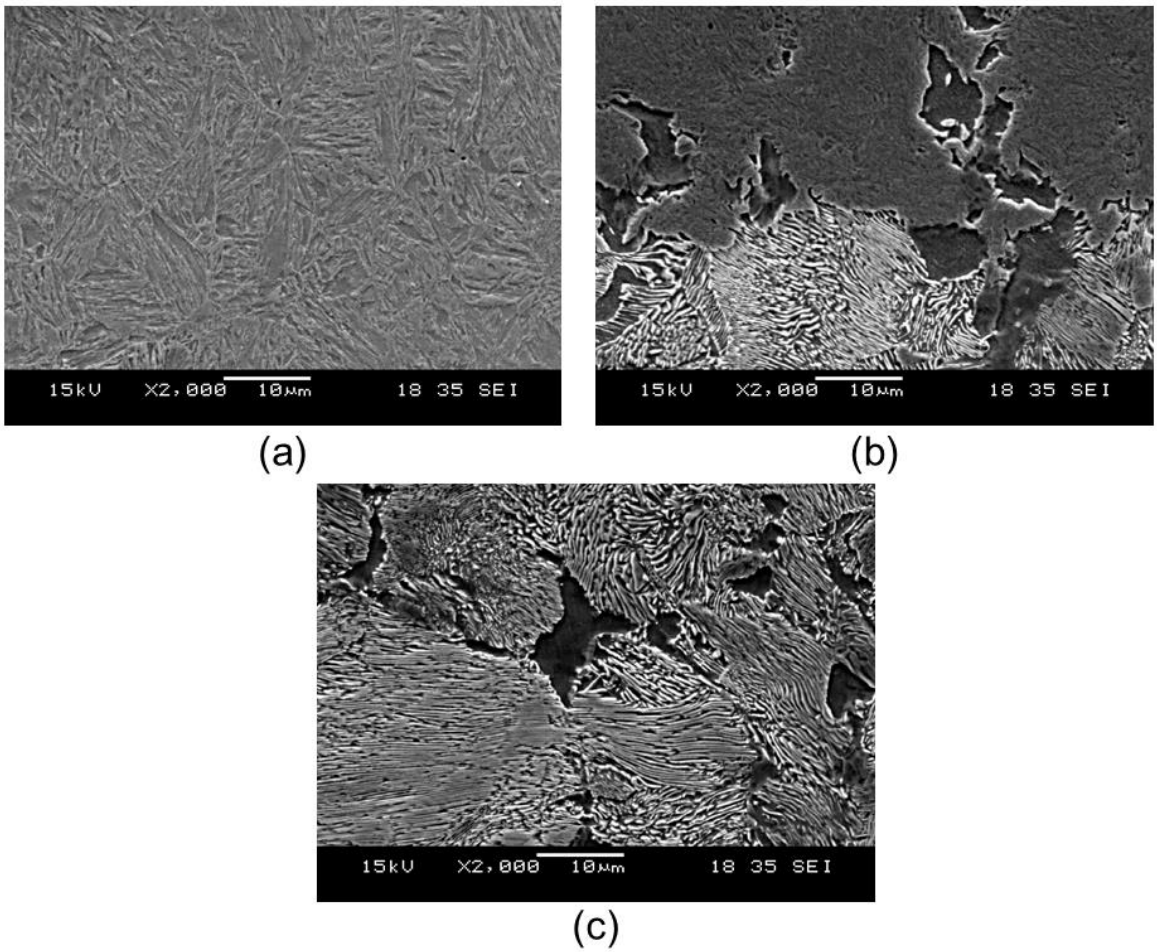

Fig. 8. Typical microstructure obtained during laser hardening under water - (a) martensitic structure near the surface; (b) mixed microstructure with undissolved ferrite in the boundary region; and (c) base microstructure with ferrite and pearlite.

The major difference between the specimens treated in air and water was the size of laser hardened zone. Figure 9 compares the depth and the width of specimens treated in air and water at different traverse speeds. Both depth and width decreased with increase in traverse speed. This is because fast speed provides short interaction time for laser beam to heat the steel surface. Therefore, the heat cannot penetrate deep into the material at fast traverse speed resulting in small laser affected area. In case of water submerged specimen, the trend is not very clear due to the zigzag nature of laser hardened track. Nevertheless, the depth and width of water submerged specimen were smaller compared to the laser treated specimen in air for all cases. This is because water attenuates the laser energy reaching the surface as discussed above.

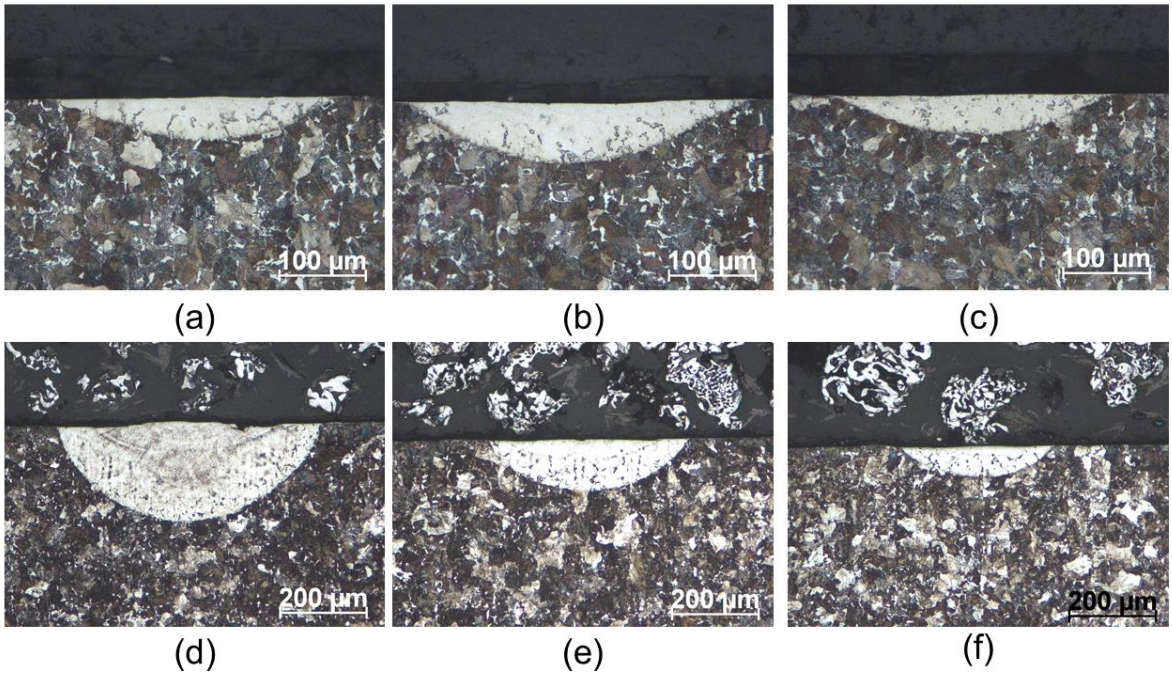

Fig. 9. Cross section micrographs of laser hardened track in water (a,b,c) and air (d,e,f) at different traverse speeds – (a,d) 10 mm/s; (b,e) 50 mm/s; and (c,f) 100mm/s. A laser power of 250 W was used for all cases.

In addition, a tempered microstructure was obtained in some specimens treated at slow traverse speed in water. Figure 10 shows the microstructure obtained at 250 W power and 1 mm/s traverse speed with 1 mm thick water layer. The tempering can be traced back to diffraction of laser beam by water layer. The slow traverse rate results in excessive heating of the water resulting in its convective motion which diffracts the incoming laser beam in random direction. Thus, the diffracted beam might temper the previously hardened microstructure. Although tempering is considered beneficial in preventing crack propagation and removing residual stresses,[16] further studies need to be carried out to verify this.

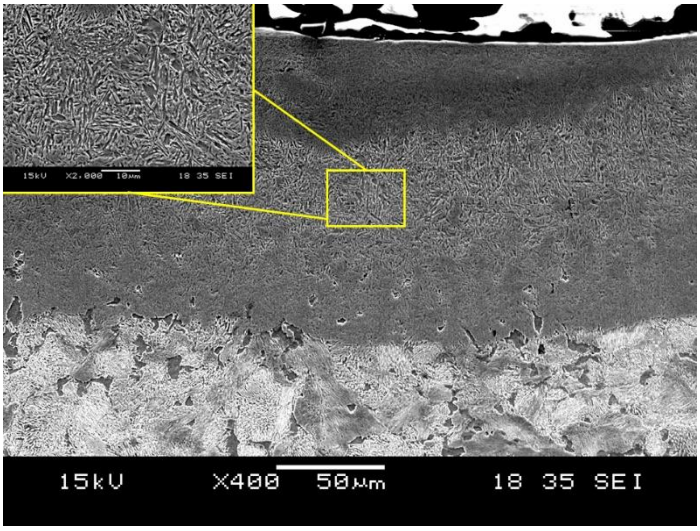

Fig. 10. A typical micrograph of laser hardened track formed at slow traverse speeds. The inset shows the magnified image of back-tempered zone.

Cross-section microhardness measurements corroborated well with the microstructure obtained. Figure 11 shows the cross-section hardness of specimen treated in both air and water at 250 W power and 10 mm/s traverse speed. As observed during surface hardness measurements, the water submerged specimen had higher hardness in the laser hardened region than in air hardened specimen. The difference in the depth of hardened zone could also be clearly appreciated from the microhardness profile. A slight reduction in hardness is found for air hardened specimen possibly due to surface decarburization. Decarburization is known to occur at steel surface despite short interaction time in laser material processing. Analysis of decarburization is out of the scope of this paper and can be found elsewhere.[17]

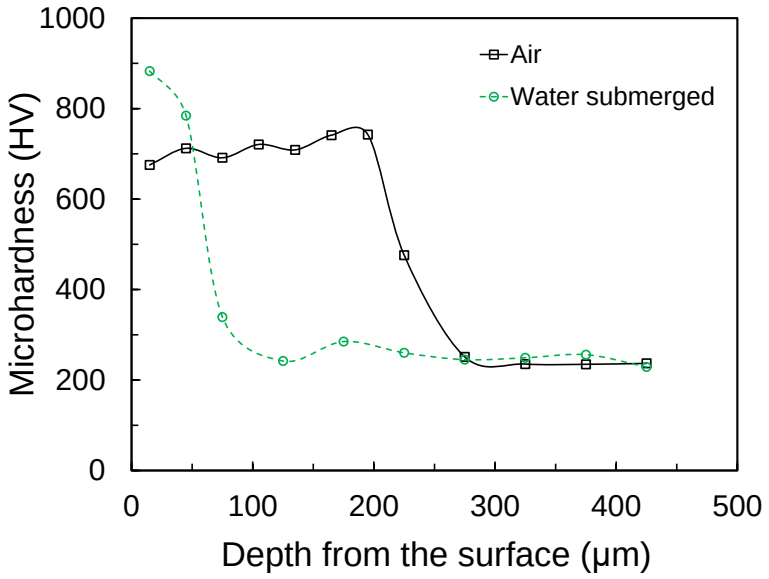

Fig. 11. Graph comparing the hardness variation along the depth for specimens treated in air and water.

The analysis therefore reveals that use of water increases the surface hardness, but significantly reduces the size of laser hardened zone. Increase in surface hardness can be attributed to the additional cooling effect by water which improves the chances of complete martensitic transformation. However, a thick water layer acts as an effective shield reducing laser energy reaching the surface. This decreases the size of laser hardened zone. Therefore, an optimum water layer of 1-3 mm is recommended if hardening is to be carried out in water submerged condition. Furthermore, corrosion and mechanical properties of the hardened surface could be explored in future studies to assess its effectivity for practical applications.

4. Conclusion

The effect of water layer during laser surface hardening has been explored based on the morphology and hardness of the hardened surface in AISI 1055 steel. The main findings are listed below:

- Water submerged laser hardening can be carried out effectively with water layer up to 3 mm above the steel surface. Higher water layer severely attenuates the laser beam reaching the surface.
- Surface oxidation is minimized but could not be completely prevented despite presence of water layer. The water motion results in random distribution of metal slag at the surface.
- As long as water depth is small enough, superior surface hardness can be achieved compared to laser hardening in air. This is attributed to rapid cooling due to presence of water. The surface hardness measured is as high as 883 HV.
- The shape of hardened track is similar as in conventional laser hardening. However, the depth and width are found to be significantly smaller than hardening in air.

Acknowledgements

This work was supported by A*STAR SINGA Scholarship, Nanyang Technological University and Advanced Remanufacturing and Technology Center (ARTC), Singapore under the Collaborative Research Project RCA-15/287.

References

1. Y. S. Tian, C. Z. Chen, D. Y. Wang and T. Q. Lei, *Surf. Rev. Lett.* **12** (2005) 123–130.

2. Y. C. Guan, W. Zhou and H. Y. Zheng, *Surf. Rev. Lett.* **16** (2009) 801–806.

3. B. Norhafzan, S. N. Aqida, E. Chikarakara and D. Brabazon, *Appl. Phys. A.* **122** (2016) 384.

4. R. Sun, Y. C. Guan and Y. Zhu, *Surf. Rev. Lett.* **23** (2016) 1630003.

5. M. Ezzat, M. A. El-Waily, M. Abdel-Rahman and Y. Ismail, *Surf. Rev. Lett.* **25** (2018) 1850079.

6. P. Xue-Long, F Han-Guang, W. Kai-Ming, S. Shu-Ting, J. Jiang, L. Jian, Y. Da-Wei, X. Zhen-Guo and L. Yong-Ping, *Surf. Rev. Lett.* (2017) 1950030.

7. A. K. Nath and S. Sarkar, *Advances in Laser Materials Processing (Second Edition)* (Elsevier, 2018).

8. G. Krauss, *Steels: processing, structure, and performance* (ASM International, 2015).

9. X. Zhang, W. Chen, E. Ashida and F. Matsuda, *J. Laser Appl.* **15** (2003) 279–284.

10. N. Guo, X. Xing, H. Zhao, C. Tan, J. Feng and Z. Deng, *Mater. Des.* **115** (2017) 112–120.

11. H. Chen, N. Guo, X. Shi, Y. Du, J. Feng and G. Wang, *J. Manuf. Process.* **31** (2018) 103–115.

12. S. S. Babu, S. A. David, J. M. Vitek and K. Mundra, *Sci. Technol. Weld. Join.* **4** (1999) 276–284.

13. K. Takahashi, H. Kobayashi and T. Yoneyama, in *Preprints of the National Meeting of JWS* **66** (2000) 70–71.

14. N. Maharjan, W. Zhou, Y. Zhou and N. Wu, in *High-Power Laser Materials Processing: Applications, Diagnostics, and Systems VII* (International Society for Optics and Photonics, 2018).

15. A. I. Katsamas, *Surf. Coatings Technol.* **201** (2007) 6414–6422.

16. X. Hu and Y. Li, *Surf. Rev. Lett.* **20** (2013) 1350048.

17. N. Maharjan, W. Zhou, Y. Zhou and N. Wu, *Appl. Phys. A.* **124** (2018) 682.